APPLICATIONS OF
MODELLING AND SIMULATION
http://arqiipubl.com/ams eISSN 2600-8084 VOL 4, 2020, 183-201

Farmland Fertility Optimization for Designing of Interconnected Multi-machine Power System Stabilizer

Aliyu Sabo[1,2*], Noor Izzri Abdul Wahab[1], Mohammad Lutfi Othman[1], Mai Zurwatul Ahlam Mohd Jaffar[3] and Hamzeh Beiranvand[4]

[1]Advanced Lightning, Power and Energy Research (ALPER), Department of Electrical and Electronics Engineering, Faculty of Engineering, Universiti Putra Malaysia, 43400 UPM Serdang, Selangor, Malaysia
[2]Department of Electrical and Electronics Engineering, Nigerian Defence Academy, PMB 2109, Kaduna, Nigeria
[3]Department of Mathematics, Faculty of Science, Universiti Putra Malaysia, 43400 UPM Serdang, Selangor, Malaysia
[4]Department of Electrical Engineering, Lorestan University, Khoramabad, Iran

[*]Corresponding author: saboaliyu98@gmail.com

Submitted 07 March 2020, Revised 08 May 2020, Accepted 11 May 2020.

Abstract: This study describes the process of interconnected multi-machine power system stabilizer (PSS) optimization using a new intelligent technique called farmland fertility algorithm (FFA) to increase the stability of IEEE three machine nine bus power system and offset the low-frequency oscillations (LFOs) during a symmetrical 100 ms three-phase fault at bus 9. The FFA-PSS controller performance is compared with two familiar classical techniques, i.e. Genetic Algorithm (GA-PSS) and Particle Swarm Optimization (PSO-PSS) to confirm the capability of the proposed technique to realize improved system stability enhancement. The Eigenvalue simulation results with FFA produce stable Eigenvalues that increase the damping ratio of the Electromechanical Modes (EMs) to more than 0.1 with smaller overshoots and time to settle which shows the effectiveness of the method for multi-machine stability improvement. Also, the phasor simulation results show that the transient responses of the system rise time, settling time, peak time and peak magnitude were all impressively improved by an acceptable amount for the interconnected system with the proposed FFA-PSS thus, was able to control the LFOs effectively and produces enhanced performance compared to the GA and PSO based PSS. Similarly, the result validates the effectiveness of the proposed FFA tuned PSS for LFO control which demonstrates robustness, efficiency, and convergence speed ability than the classical GA and PSO tuning methods.

Keywords: Farmland fertility algorithm; Genetic algorithm; Low-frequency oscillation; Particle swarm optimization; Power system stabilizer.

1. INTRODUCTION

Interconnected multi-machine power systems are complicated due to several nonlinear dynamic devices and components associated with their interconnections in supplying the required energy to the consumers. In an event of any disturbances, the interconnected synchronous generators in the system will oscillate and may cause the system to lose synchronism [1]. Power system oscillations (PSOs) in the range of low frequencies possess a significant impact on the system dynamic stability [1-2]. To improve the PSOs damping characteristics and increase the system oscillation stability, automatic voltage regulator (AVR) alone in the generator excitation system is not enough [4]. Therefore, the utilities equipped the exciter with additional supplementary control which is simple in structure, an effective and economical technique called power system stabilizer (PSS). Conventional PSS is one of the many essential power system components which have been broadly used to suppress out low frequency oscillation (LFO) during contingencies and improve the system stability.

Generally, the conventional PSS is a fixed parameter type under a specific operating condition and its parameters were obtained based on trial and error method. These have a considerable effect on its performance and may not effectively damp out the LFO in the system. Conventional PSS parameter design problem is a cumbersome exercise where many analytical methods were proposed in the literature like the eigenvalue method, gradient methods for optimization, numerical programming method, robust control method, H_∞ method and so on [1-2]. However, it was reported that, for the design of PSS for interconnected multi-machine systems operating on different conditions and configurations, these numerical methods involve representing the system mathematical models that are difficult for a large system. Also, the application of the numerical methods involves large computation stress which consumes excessive time, and the convergence rate is slow [7]. Another limitation with these approaches is, they are unable to reach a global solution [5] [8]. It is usually hard to find online optimal controller parameters with classical tuning controller methods due to the complexity and dynamical nature of the system.

Recently, intelligent metaheuristic optimization technique has grown and gained attention due to its superiority in solving complex high dimension, non-linear, non-differentiable, non-convex, and multi-modal real-world problems [9] [10]. Various metaheuristic optimization technique such as Differential Evolution (DE) [11], Genetic Algorithm (GA) [12], Particle Swarm Optimization (PSO) [13], Whale Optimization Algorithm (WOA) [14], Salp Swarm Algorithm (SSA) [15], Kidney-inspired Algorithm (KA) [16], Grasshopper Optimization Algorithm (GOA) [5], Bacteria Foraging optimization (BF) [17], Sine Cosine Algorithm (SCA) [18], Bat Algorithm (BA) [19], Cuckoo Search Optimization (CSO) [20], Artificial Bee Colony (ABC) [21], General Relativity Search Algorithm (GRSA) [22] and others were developed for multi-machine PSSs design. These algorithms provide good performance into the problem of PSSs design. However, when the optimization objective function is multimodal with a high dimension, then the global optimum solution can have a considerable effect and the solution may be confined in local optimum points. Therefore, optimal PSSs design study for highly nonlinear interconnected multi-machine power systems under dynamic operating points is still needed for the system robust operation.

In this work, the latest optimization method called Farmland Fertility Algorithm (FFA) proposed by [23] is employed for the first time to solve optimal interconnected multi-machine PSSs design problems to test its capability and robustness and to improve on the existing GA and PSO optimization approach in stabilizer design. The GA and PSO well-known conventional optimization methods provide good performance in PSS design but in most cases stuck in local optimum point and has a slow convergence rate. This motivation is behind the application of FFA in this regard. The FFA is a descriptive nature-inspired method of optimization where farmers divide their farm environment into several parts based on the farm soil quality and were recently successfully applied in [24] for the optimal design of grid-connected hybrid renewable energy system with fuel cell storage in Ataka, Egypt. This optimization technique is new for power system [24] and it have been employed to improve the multi-machine power system damping properties. For the FFA-PSS, results were found to be able to optimize the PSS parameters and able to develop the unstable modes as the system realizes stability with small overshoot. Section 2 presents the system model studies while section 3 and 4 explains the research results and conclusion respectively.

2. SYSTEM MODEL STUDIED

2.1 Test System Modeling

Differential-Algebraic Equations (DAEs) define the test system model dynamism. The m synchronous machine differential equations and the automatic voltage regulator (AVR) [25], are defined by the following equations:

$$T'_{d0i}\frac{dE'_{qi}}{dt} = E_{fdi} - E'_{qi} - (X_{di} - X'_{di})I_{di} \tag{1}$$

$$T'_{q0i}\frac{dE'_{di}}{dt} = -E'_{di} - \left(X_{qi} - X'_{qi}\right)I_{qi} \tag{2}$$

$$\frac{d\delta_i}{dt} = \omega_i - \omega_s \tag{3}$$

$$\frac{2H_i}{\omega_s}\frac{d\omega_i}{dt} = T_{Mi} - E'_{di}I_{di} - E'_{qi}I_{qi} - \left(X'_{qi} - X'_{di}\right)I_{di}I_{qi} - D_i(\omega_i - \omega_s) \tag{4}$$

$$T_{Ai}\frac{dE_{fdi}}{dt} = K_{Ai}(V_{refi} - V_i) - K_{Ai}E_{fdi} \tag{5}$$

where generator rotor angle is δ, generator speed is ω, synchronous speed is ω_s, internal transient voltages are E'_d and E'_q, and they are behind X'_d and X'_q which are the d-axis and q-axis transient reactance's respectively. I_d and I_q are d-axis and q-axis constituents of the generator stator currents respectively, damping coefficient is D, mechanical power input is T_M, generator inertia constant is H, d-axis and q-axis reactance are X_d and X_q respectively. T'_{d0} and T'_{q0} are the open circuit d-axis and q-axis time variable constants respectively, V is terminal voltage for the synchronous generator, exciter voltage is E_{fd}, regulator gain is K_A, regulator time constant is T_A while regulator reference voltage is V_{ref}. For i in Equations (1) and (4) represent the ith synchronous generator.

To simplify the excitation controller design, we consider the mechanical input torque T_{Mi} as a constant term meaning we make an assumption here that the governor action to be very slow that its impact is insignificant on the system dynamics [22]. Now the electrical torque is expressed as:

$$T_{Ei} = E'_{di}I_{di} + E'_{qi}I_{qi} + \left(X'_{qi} - X'_{di}\right)I_{di}I_{qi} \tag{6}$$

The electrical torque is put in Equation (4). For a power system having n buses and m generators, it provides $m - n$ load buses, then the algebraic power system equations can be represented by:

$$0 = V_i e^{j\theta i} + (R_{si} + jX'_{di})\left(I_{di} + jI_{qi}\right)e^{j\left(\delta i - \frac{\pi}{2}\right)} - \left[E'_{di} + \left(X'_{qi} - X'_{di}\right)I_{qi} + jE'_{qi}\right]e^{j\left(\delta i - \frac{\pi}{2}\right)}\ i = 1, \cdots, m \tag{7}$$

$$V_i e^{j\theta i}\left(I_{di} + jI_{qi}\right) + P_{Li}(V_i) + jQ_{Li}(V_i) = \sum_{k=1}^{n} V_i V_k Y_{ik}\, e^{j(\theta i - \theta k - \alpha ik)}, i = 1, \cdots, m \tag{8}$$

$$P_{Li}(V_i) + jQ_{Li}(V_i) = \sum_{k=1}^{n} V_i V_k Y_{ik}\, e^{j(\theta i - \theta k - \alpha ik)}, i = m+1, \cdots, n \tag{9}$$

where active and reactive powers are P_L and Q_L respectively, the admittance matrix is $Ye^{j\alpha}$ and the bus voltage angle is θ. From Equation (8), V_i is the voltage regulator input voltage which is automatically defined via the network algebraic constraints. Also the functions $P_{Li}(V_i)$ and $Q_{Li}(V_i)$, the $n + m$complex algebraic equations must be solved for V_i, θ_i $(i =$

$1, \cdots, m$) and I_{di}, $I_{qi} (i = 1, \cdots, m)$ in terms of the states δ_i, E'_{di}, E'_{qi} $(i = 1, \cdots, m)$. The currents can be explicitly eliminated by solving either Equation (7) or (8) and substituting into the differential equations and remaining algebraic equations. Therefore, this would leave only n complex algebraic equations to be solved for the n complex voltages$V_i e^{j\theta i}$. Constant impedances in a power system having m generators represent the loads. V_i and V_k for Equations (8) and (9) are the voltage regulator input voltage and the ik^{th} the entry of the network bus admittance matrix. Multi-machine two-axis model type of network was used to validate this method.

To reduce the element of the load in the admittance matrix of the power lines, the order reduction method is used. Consider a power system linear model in Equation (10).

$$\triangle \dot{x} = Cx + D\mu \tag{10}$$

where the system state variables vector is x, C is the system state matrix, D is the system input matrix and μ is the control input vector. Equations (1) – (9) determine the nonlinear dynamic behavior of the electric power system. These equations are solved using an ordinary differential equation (ODE) solver using a solution loop in the SIMULINK.

2.2 PSS Design Procedure

A widely speed based conventional PSS lead-lag structure and IEEE-type-ST1 excitation system shown in Figure 1 are utilized in this research [26]. The conventional PSS can be represented by the transfer function of ith system as:

$$G_i(S) = \frac{V_{PSSi}(S)}{d\omega_i(S)} = KG_i \frac{sT_w}{1+sT_w} \frac{(1+sT_{1i})}{(1+sT_{2i})} \frac{(1+sT_{3i})}{(1+sT_{4i})} \tag{11}$$

Here, V_{PSSi} is the stabilizing signal from the conventional PSS output at the ith machine, T_w is called the time constant from the washout block, $d\omega_i$ is the mechanical speed deviation signal from the synchronous speed of the ith machine. The PSS parameters to be determined here are the stabilizer gain KG_i and the T_{1i}, T_{2i}, T_{3i} and T_{4i} respectively. LFO are usually perceived in power angles variations, mechanical rotor speeds, and also active and reactive line powers. To establish an objective function will be to minimize any of these variations in the system.

To increase the damping properties of the electromechanical modes (EMs), there are two types of objective function used for the optimization process, the Eigenvalue-based objective function Equation (12) which is employed to prevents unstable modes formation that will lead the system eigenvalues moving towards the left-hand side (LHS) of the complex plane while Time-domain based objective function is the other type. In this study, the damping properties of the electromechanical modes (EMs) was improved using an Eigenvalue-based objective function in Equation (12) where the PSS control parameters can be determined by solving the system state matrix C from Equation (10).

$$J_{egn} = \max\{real(\lambda_i) | \lambda_i \in EMs\} + P_F \sum\{real(\lambda_j) | \lambda_j > 0\} \tag{12}$$

$$EMs = \left\{(\lambda_k) | 0 < {}^{im(\lambda_k)}/_{2\pi} < 5\right\} \tag{13}$$

where λ_i represents the i-th eigenvalues of the power system state matrix C from Equation (10), P_F is a penalty constant that is applied in forming the positive eigenvalues (and also can improve the slow eigenvalues) and is considered to be 50 in this study. The objective function J_{egn} minimizes the inter-regional and EMs system damping and at the same time prevents unstable modes formation that will lead the system eigenvalues moving towards the left-hand side (LHS) of the complex plane. The typical values of the optimized parameters of the PSS gain are $0.001 \leq KGi \leq 50$ and $0.001 \leq T1i \leq 1$, $0.02 \leq T2i \leq 1$, $0.001 \leq T3i \leq 1$, $0.02 \leq T4i \leq 1$ for the time constants of the PSS. Also, the value of washout time constant is commonly fixed and chosen $T_w = 10$ [22]. The proposed novel FFA optimizer computes the optimization problem and search the optimum values of PSS parameters, $\{KG_i, T_{1i}, T_{2i}, T_{3i}, T_{4i};\ i = 1, 2, \cdots, n_{PSS}\}$.

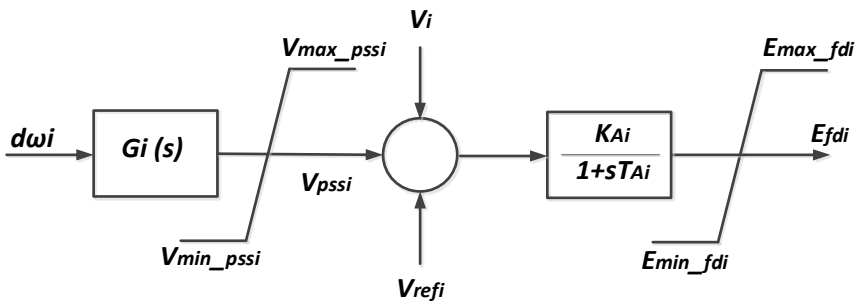

Figure 1. Conventional PSS connected to IEEE-type-ST1 excitation system

2.3 Farmland Fertility Algorithm Description

A new optimization technique called Farmland Fertility Algorithm (FFA) [23] is proposed in this study for the optimal design of the PSS damping controller for mitigation of LFOs of an interconnected multi-machine power system. Farmers divide their farmland into several space base on the concept of FFA optimizer to assess soil quality in each farm environment space. There will be soil quality differences in the farmland space because the soil quality variation relies on adding some special constituent materials to the soil. In this case, the farmers used different additive constituents to optimize the quality of the farmland. However, adding these constituents to the farmland soil may optimize or may not optimize the soil quality. Therefore, farmers used their farming know-how on each soil type to determine these materials in improving the soil quality farmland [23]. The farmers do this continuously by acquiring more experience with the soil quality using the earlier optimized results acquired. FFA application for optimization is new for the power system. Its capability is highly plausible matched to other nature-inspired optimization methods [23].

FFA optimization process for determining the best soil quality and the best addictive materials for improving the soil quality is mathematically highlighted out in the following phases:

2.3.1 Initialization

Like other metaheuristic approaches, FFA approach starts by creating an initial random population based on the following measures:

- Taking the number of farmland sections into consideration (number of farmland divided sections for optimization problem) expressed by k.
- Considering the number of available solutions in each farmland section (number of existing solutions in each farmland section) expressed by n.

Mathematically, a total number of populations N is denoted by Equation (14) where k is an integer number greater than zero and is denotes the number of sections for the optimization problem. The optimization problem defines the standard number of farmland sections therefore, the entire optimization search space is divided into k sections in which each section has a specific number of solutions.

$$N = k * n \tag{14}$$

The number of existing solutions in each farmland section or the number of available solutions in each search space section is denoted by an integer number n. Random production of search space considering the upper (U_j) and lower (L_j) boundaries of variable x are given by Equation (15).

$$x_{ij} = L_j + rand(0,1) * (U_j - L_j) \tag{15}$$

where $j = [1 \cdots D]$ denotes the variable x dimension in the optimization problem which is based on the total number of population and is equal to $[1 \cdots N]$.

In this paper, x represents the 10 PSSs design parameters (the two PSS gains and the 8 lead-lag PSSs time constants respectively) which is required to be determined. FFA main problem is the k variable which differentiates the proposed algorithm from other metaheuristics techniques. As farmers divide their farmland area, k is considered for the partitioning of the search space. In a real-world application, farmers divide their environment from other lands in a square or rectangular shape. The author in [23] explains that if the k value is chosen above 8, then the FFA search engine will be stuck in the local optimal, therefore, in this work, k value is chosen base on trial and error to reach optimal solution and is taken between 2 and 8.

2.3.2 Soil Quality Determination for Each Section of the Farmland

After getting the total number of the initial population and generating the initial population from Equation (14) and Equation (15) respectively, this stage evaluates the fitness of all the existing solutions in the search space which mathematically, the quality of the soil in each section of the search space can be given by Equation (16) and Equation (17) respectively. Each farmland section quality is obtained by the average of the existing solutions in each farmland section.

$$section_s = x_{(aj)}, a = n * (s-1) : n * ss = \{1, 2, \cdots k\}, j = \{1, 2, \cdots 4\} \tag{16}$$

Equation (16) separates each farmland section available solutions so that we can compute the average of each separately. From Equation (16), x represents to all the solutions in each search space while s denotes the number of section and $j = [1 \cdots D]$ explains the variable x dimension.

$$Fit\_section_s = Mean\left(all\ Fit(x_{ji})\ in\ section_s\right). s = \{1, 2, \cdots k\}. i = \{1, 2, \cdots n\} \tag{17}$$

From Equation (17), $Fit\_section_s$ represents the quality of solutions for each farmland section where each section has a special amount of quality and in the search space is the average fitness of all available solutions in each farmland section. Therefore, for each of the farmland sections, a total average of the solution is achieved within it and is stored in $Fit\_section_s$ space. Finally, this stage determines the fertility of each farmland section, their solutions, and the average of each section.

2.3.3 Updates the Memories

After acquiring the solutions and average of each farmland section, this stage updates the local and global memories of each farmland section. Among the solutions, best solution cases of each section are saved in the local memory while the best solution cases of all farmland sections are saved in the global memory which is obtained by the number of best local memory expressed in Equation (18) and for the best global memory expressed in Equation (19).

$$M_{local} = round(t * n),\ 0.1 < t < 1 \tag{18}$$

$$M_{Global} = round(t * N),\ 0.1 < t < 1 \tag{19}$$

where M_{local} and M_{Global} are the number of solutions stored in the local and global memory respectively. These solutions are stored based on their fitness and correctness in these memories and at this stage are updated in both memories. Among these solutions, the best and worst parts are determined and the algorithm engine enters the next stage.

2.3.4 Changing the Soil Quality in Each Farmland Section

After obtaining the quality of each of the farmland section given by Equation (17), the parts of the farmland that has the worst quality will be changed by this stage. Equation (16) already determines the number of solutions for each farmland part. The concern about the quality of the worst section of the farmland is solved by combining all the existing solutions in the worst part of farmland with one of the available solutions in the global memory. This is expressed in Equation (20) and (21).

$$h = \alpha * rand(-1, 1) \tag{20}$$

$$X_{new} = h * \left(X_{ij} - X_{MGlobal}\right) + X_{ij} \tag{21}$$

From Equation (21), $X_{MGlobal}$ defines a random solution among the existing solutions in the global memory while α denotes a number between 0 and 1 that should be initialized at the beginning of the FFA search. The solution of the worst part of the farmland that is chosen to make the changes is X_{ij} while h represents a decimal number that is obtained from Equation (20). Equation (21) will finally give a new solution that can be applied to make the necessary changes to the search. After making the changes in the worst section of the farmland, other sections should be combined with available solutions in the whole search space. Equations (22) and (23) can then be applied to determine the available solutions in the other farmland sections.

$$h = \beta * rand(0, 1) \tag{22}$$

$$X_{new} = h * \left(X_{ij} - X_{uj}\right) + X_{ij} \tag{23}$$

From Equation (23), X_{uj} defines a random solution among the existing solutions in the whole search space. This means that between all solutions in the farmland parts a selected random solution is chosen. A number between zero 0 and 1 is β and it is initialized only at the beginning of the FFA search. The solution relating to sections beside the worst farmland section that is chosen to make the necessary change to the algorithm is X_{ij} while h represents a decimal number that is obtained from Equation (22). Equation (23) will finally give a new solution that is obtained by the necessary applied changes to the search algorithm.

2.3.5 Soil's Combination

In this stage, the farmers decide to combine each soil within the partition farmland base on the best available cases in their local memory i.e. $Best_{Local}$ at the last stage. There is a provision about combining the best in local memory so that, not all available solutions are combined with local memory in all farmland sections. This stage makes sure some of the available solutions in all places are combined with the best solution ever found $Best_{Global}$ to enhance the quality of the existing solutions in each farmland section. The combination of the considered solution with $Best_{Local}$ or $Best_{Global}$ can be obtained from Equation (24).

$$H = \begin{cases} X_{new} = X_{ij} + \omega_1 * \left(X_{ij} - Best_{Global}(b)\right) & Q > rand \\ X_{new} = X_{ij} + rand(0, 1) * \left(X_{ij} - Best_{Local}(b)\right) & else \end{cases} \tag{24}$$

From Equation (24), two methods may produce a new solution. The variable Q determines the amount of combination of solutions with $Best_{Global}$ and is a number between zero 0 and 1 that must be obtained in the initial stage of the search engine. The variable ω_1 represents the farmland fertility which is an integer and should be determined at the initial stage of the search engine. Its value decreases according to the repetition of the search algorithm as shown in Equation (25). X_{uj} defines a solution to apply that make the changes selected from all farmland sections while X_{new} defines a new solution obtained according to the applied changes.

$$\omega_1 = \omega_1 * R_v\ , 0 < R_v < 1 \tag{25}$$

2.3.6 The Final Conditions

In this stage, the available solutions in the search space are evaluated based on the objective function of the design problem. In this work, an Eigenvalue-based objective function is used based on WSCC test power system dynamics following a symmetrical three-phase fault as an objective function of the design problem. Regardless of the number of partitioned farmlands, this stage performed all existing available solutions in the search space thus, the fitness and correctness of each existing available solutions are obtained. This stage is the final stage for searching the final conditions in the search space and if the condition is found optimal, the FFA engine ends otherwise it continues until the final condition is achieved. Figure 2 explains the step by step flowchart stages for FFA optimization process for determining the best soil quality and the optimal additive constituents for optimizing the soil quality.

The PSSs design optimization problem is to minimize the objective function of Equation (12) and determine the optimal PSS parameters of the Synchronous generators 2 and generator 3 respectively. In this work, the proposed FFA algorithm for PSSs design operates according to the following steps:

a) Run the program of PSSs design based on the test system considered and the fault subjected to it.
   - Generate the initial population, Equation (15).
   - Run the program of PSSs design from Equations (1) – (9).
   - Evaluate the objective function for all portions, Equations (12) and (13).

b) Run the optimization algorithm with PSSs in the test system based on Equations (16) - (23) by the following process:
   - Update the positions and the optimum PSSs parameters based on the nature of the FFA optimizer.
   - Run the program of PSSs design from Equations (1) – (9).

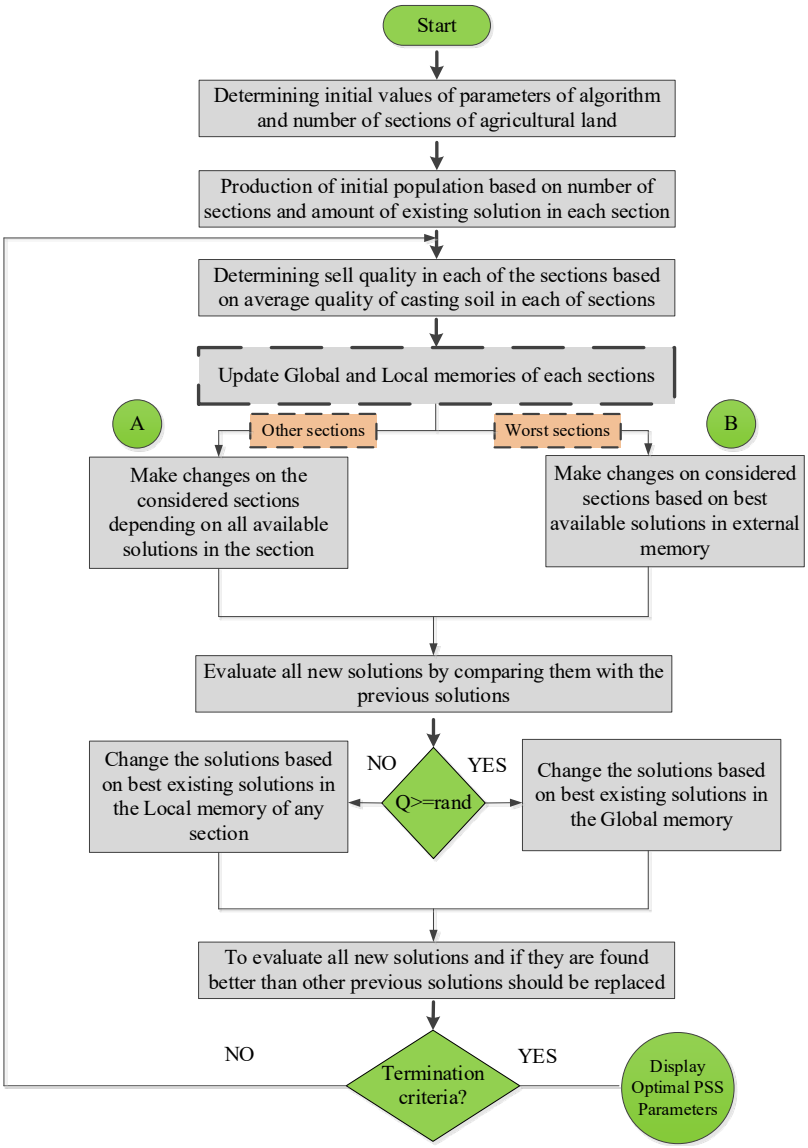

Figure 2. Farmland fertility algorithm flowchart

- Evaluate the process of the objective function for all portions, Equations (12) and (13).
- Check if the proposed system meets the flowchart criterion. If NO, then repeat the previous three processes. If YES, then stop the program and move to the next step.
- Display the PSSs optimal parameters.

Figure 3 shows the description flowchart of the PSS design via the proposed FFA method with the interconnected multi-machine power system while Figure 4 shows the proposed FFA-PSS closed loop structure with the interconnected multi-machine power system. Table 1, Table 2 and Table 3 show the suitable choice of parameters used for the GA, PSO, and the proposed FFA algorithms which helps the algorithms achieved optimal convergence speed and fast computational cost. The optimization process was terminated by a pre-specified number of iterations for all the three algorithms and it is worthy to mention that all the three methods were initialized and run for several numbers of times before the optimal parameters of the PSSs were chosen.

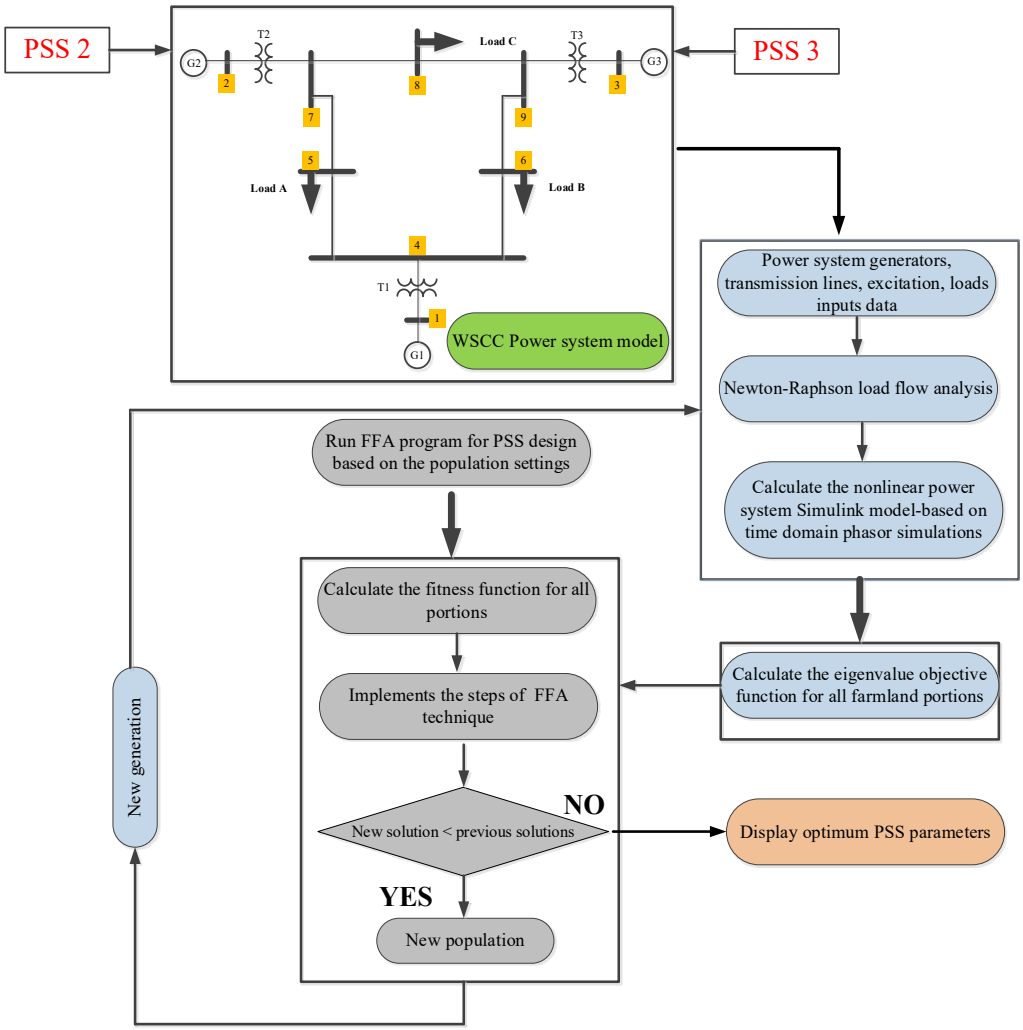

Figure 3. FFA Flowchart for PSS design with the interconnected multi-machine power system

Table 1. Search parameter settings for the GA algorithm

Parameters	GA
Number of individuals	20
Linear crossover	0
Crossover probability	0.9
Mutation probability	0.1
Total number of iterations	100

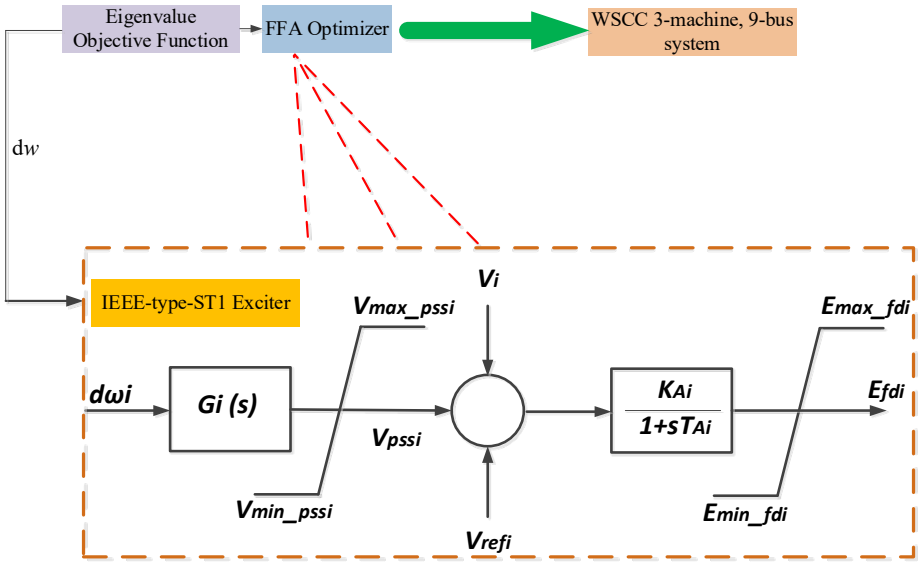

Figure 4. Structure of proposed FFA-PSS with the interconnected multi-machine power system

Table 2. Search parameter settings for the PSO algorithm

Parameters	PSO
Number of swarms	20
$c_1 = c_2$	2
w	0.8
Total number of iterations	100

Table 3. Search parameter settings for the FFA algorithm

Parameters	FFA
Number of farmland sections k	2
Number of solutions in each farmland sections n	50
Population size $Npop = k * n$	100
Alpha α	0.6
Beta β	0.4
w	1
Q	0.5
Total number of iterations	100

3. SIMULATION RESULTS AND DISCUSSIONS

This work considered the familiar Western System Coordinated Council (WSCC) three machine nine bus power system. The single line configurations of the power system are as shown in Figure 5 and the complete system data can be found in [27]. The dynamic stability of the WSCC test system can be obtained considering generator G1 (which is the slack bus) as the reference generator which is not equipped with the PSSs. The interconnected synchronous generators are represented by fourth-order models of the DAEs explained by the test system modelling equations described earlier.

In this research, MATPOWER software is utilized to execute the system power flow which computes the system's initial condition states. The solution of the DAEs Equation (1) - (9) shows the power system nonlinear dynamic behavior and the DAEs are solved via an ODE solver in MATLAB/SIMULINK. For the PSSs design, two different conditions were observed which are the base case and the system case under symmetrical three-phase fault condition. A symmetrical 100 ms three-phase fault at bus 9 i.e. at the end of transmission lines 8 and 9 were observed at $t = 1$ s and a nonlinear time-domain simulation was performed. The symmetrical three-phase fault at bus 9 for the WSCC test system was initiated when executing the system power flow which computes the system's initial condition states using MATPOWER software in the MATLAB environment. The rate at which the PSSs design index converges is shown in Figure 6 while the optimal parameters of the designed PSSs are shown in Table 4. From the convergence characteristics, the FFA method shows a better convergence rate (41 iterations) than PSO (with 84 iterations) and GA (with 96 iterations). Table 5 shows the computation time of the test power system results with the FFA method having less simulation time in locating the global solution than the PSO and the GA algorithms.

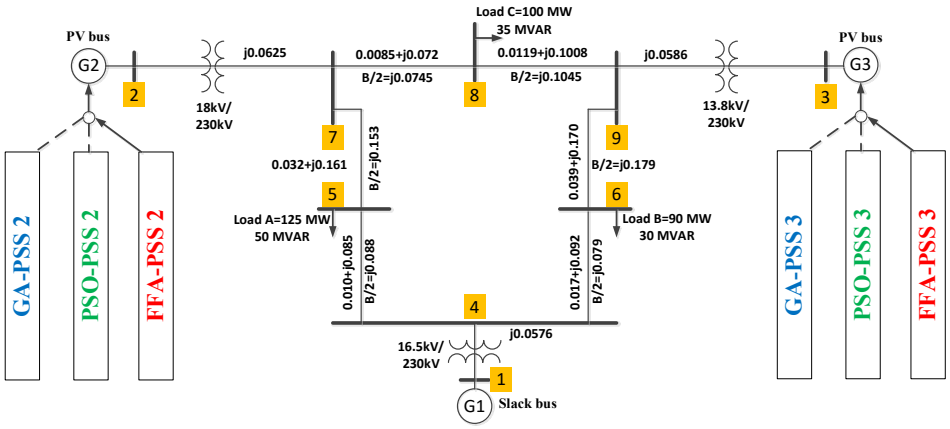

Figure 5. WSCC 3-machine power system single line structure with PSS design algorithms

Table 4. Optimal PSS parameters using three algorithms

Generator	Algorithms	K_G	T_1	T_2	T_3	T_4
G2	GA	2.5229	0.5061	0.0173	0.8007	0.0247
	PSO	4.7686	0.2605	0.0267	0.9220	0.0130
	FFA	**3.1490**	**0.6577**	**0.0166**	**0.9622**	**0.0259**
G3	GA	4.3078	0.4769	0.0208	0.6110	0.0226
	PSO	0.8432	0.1898	0.0183	0.6756	0.0225
	FFA	**0.6395**	**0.8330**	**0.0221**	**0.5589**	**0.0171**

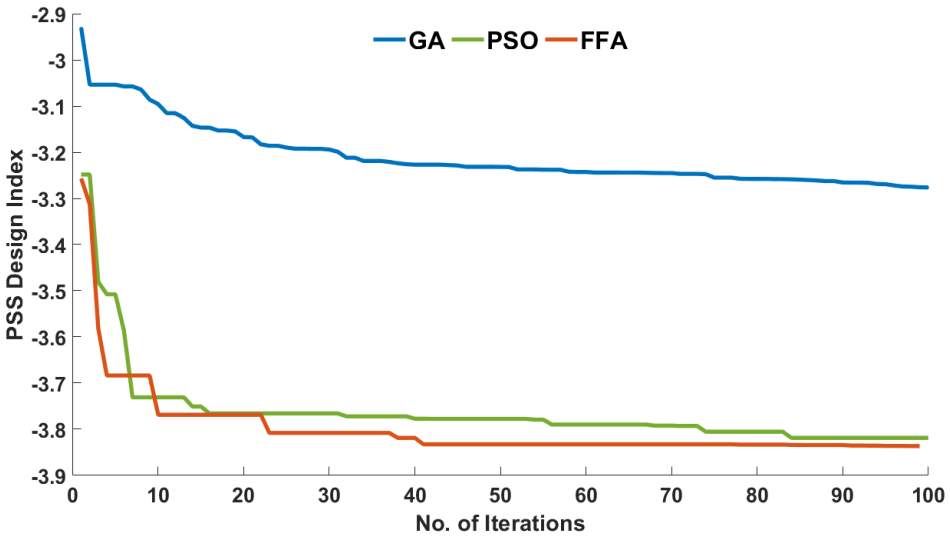

Figure 6. Convergence characteristics of PSO, GA, and FFA in finding optimal design of PSSs

Table 5. Computational cost

Algorithms	Convergence Iterations	Convergence Time (sec)
GA	96	12.096
PSO	84	10.584
FFA	**41**	**5.166**

This clearly illustrates the performance of FFA in providing faster convergence for seeking the optimal PSS parameters. Also, the system using the FFA method utilized less simulation time thus, it is found more feasible than the system employing PSO or GA methods for online optimization with fast speed processors.

3.1 Eigenvalues Analysis and Simulation Results of the Interconnected Test Power System

The robust design of PSSs performance in a power system is assessed via eigenvalue analysis. Table 6 shows the eigenvalues results while their associated damping ratio and frequency are obtained in Table 7 for the power system case without the PSS installed and the case with PSS installed in the system. From Table 6, Mode 1, and Mode 2 produce a weak damping ratio for the base case condition. After the optimal PSS design, these modes were impressively enhanced from $-0.6856 \pm 12.7756i$ and $-0.1229 \pm 8.2867i$ to $-4.0720 \pm 13.1963i$ and $-4.4351 \pm 7.3550i$ respectively using the FFA design method. Similarly, the worst damping ratio EM was improved from 0.0148 to 0.4442 using the FFA design method. Similarly, Figure 7 illustrates the eigenvalues plot comparison for the system without the PSS controller and with the proposed FFA-PSS controller based on the numerical simulation results of Table 6 and Table 7. From Table 6 and Figure 7, it is clear that the FFA-PSSs will robustly control the power system LFOs that is due to the EMs in the system.

Table 6. WSCC interconnected test power system eigenvalues

Mode	No PSSs	GA-PSS	PSO-PSS	**FFA-PSS**
1	$-0.6856 \pm 12.7756i$	$-5.8135 \pm 14.0335i$	$-5.5198 \pm 13.8009i$	$-4.0720 \pm 13.1963i$
2	$-0.1229 \pm 8.2867i$	$-3.7725 \pm 8.8008i$	$-3.5568 \pm 8.4261i$	$-4.4351 \pm 7.3550i$
3	$-2.3791 \pm 2.6172i$	$-3.4448 \pm 2.9140i$	$-3.7227 \pm 2.5912i$	$-3.7558 \pm 2.9100i$
4	$-4.6706 \pm 1.3750i$	$-3.6222 \pm 2.4747i$	$-3.5777 \pm 2.7425i$	$-3.1817 \pm 2.3440i$
5	$-3.5199 \pm 1.0156i$	$-3.3773 \pm 2.08156i$	$-3.5649 \pm 2.2191i$	$-3.9629 \pm 2.5614i$

Table 7. WSCC interconnected power system damping ratio and frequency of eigenvalues

No PSSs		GA		PSO		**FFA**	
Damping Ratio	Frequency	Damping Ratio	Frequency	Damping Ratio	Frequency	Damping Ratio	Frequency
0.0536	2.0333	0.3379	2.2673	0.3478	2.2743	0.3200	2.1417
0.0148	1.3189	0.4417	1.2711	0.4274	1.2007	**0.4442**	1.2706
0.6726	0.4165	0.8177	0.4333	0.8227	0.4138	0.7943	0.4223
0.9593	0.2188	0.8449	0.3965	0.8427	0.3947	0.8625	0.3731
0.9608	0.1616	0.8862	0.3140	0.8824	0.3321	0.8851	0.3285

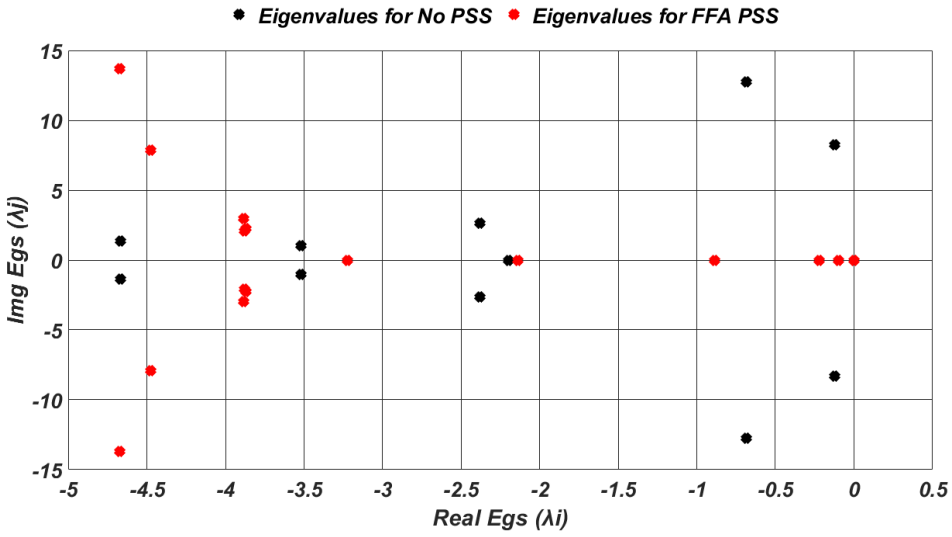

Figure 7. Eigenvalues plot comparison for the system without PSSs damping controller and with FFA-PSS damping controller

3.2 Time-Domain Simulation of the Interconnected Test Power System

To achieve a robust PSSs design in the power system, after eigenvalues simulation analysis, nonlinear time-domain simulations should be done on the system for final evaluation. Two different conditions were observed which are the case where the system is subjected to a three-phase fault without PSSs damping controller and the case where the system is subjected to a three-phase fault with PSSs damping controller. A symmetrical 100 ms three-phase fault at bus 9 i.e. at the end of transmission lines 8 and 9 were observed at $t = 1$ s and a nonlinear time-domain simulation was performed. After the fault is cleared at 0.2 s, the system stable condition was restored.

3.2.1 Parameter estimation via three-phase fault without PSS study

In this section, the system undergoes a disturbance without a damping controller (PSSs) for LFOs mitigation and hence the system stability enhancement. Nonlinear time-domain simulation was performed and Figure 8 shows the unstable generator power angles δ relative to δ_1 in radian for the interconnected test power system for the base case condition while Figure 9 shows unstable the generator field voltage E_{fd} in volts for G_1, G_2 and G_3 base case system condition respectively. Similarly, Figure 10 shows unstable the system active power response P_e in per unit for G_1, G_2 and G_3 respectively while Figure 11 shows the unstable system rotor speed response ω in radian per seconds for G_1, G_2 and G_3 respectively.

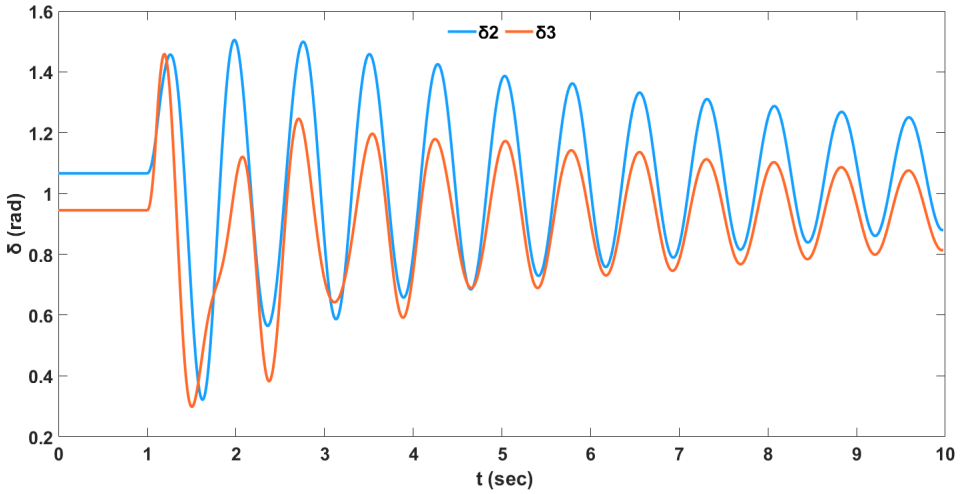

Figure 8. Unstable relative power angle response w.r.t to δ_1 of the interconnected power system for a three-phase contingency at bus 9 without PSSs

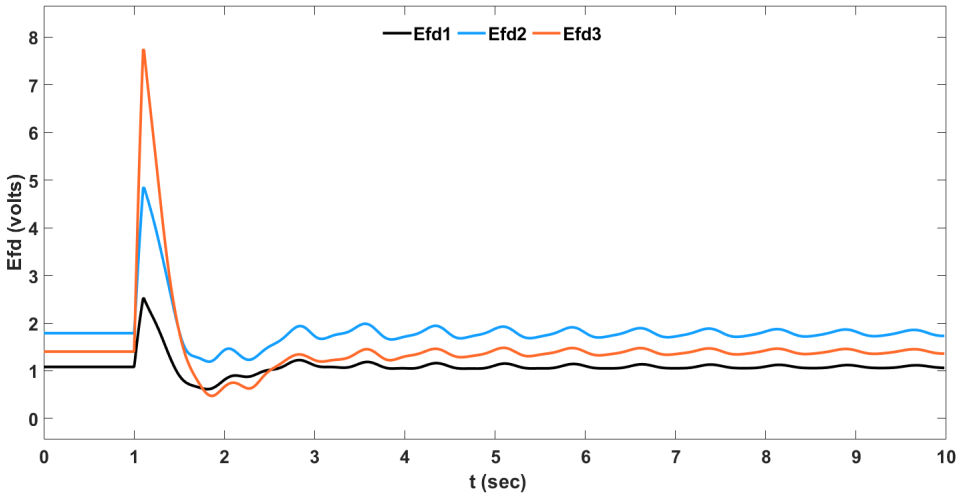

Figure 9. The unstable field voltage response of the interconnected power system for a three-phase contingency at bus 9 without PSSs

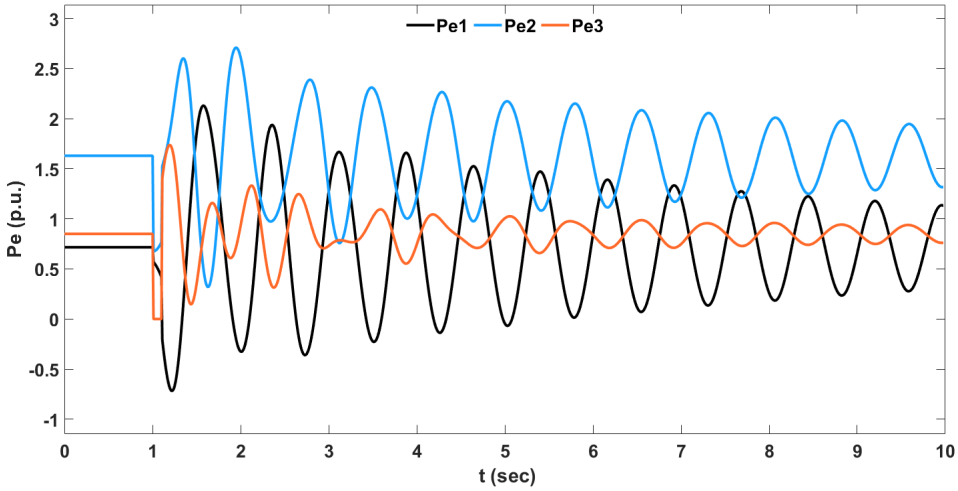

Figure 10. Unstable active output power response of the interconnected power system for a three-phase contingency at bus 9 without PSSs

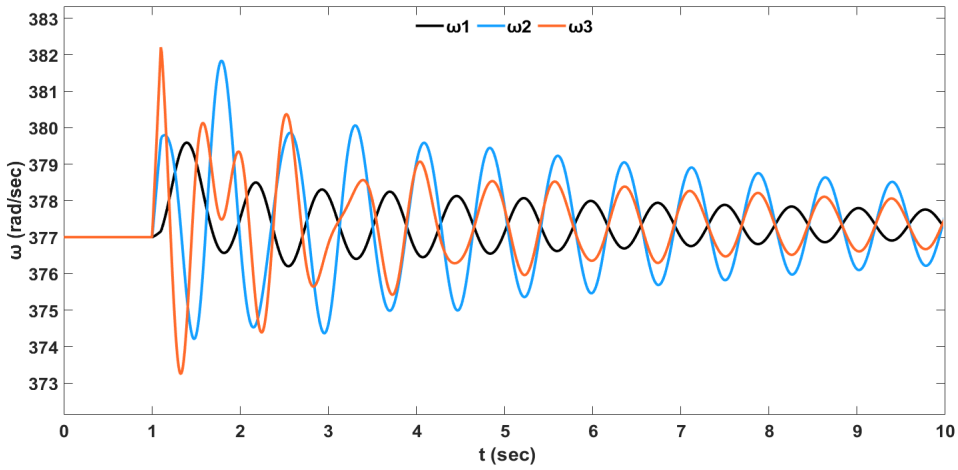

Figure 11. Unstable rotor speed response of the interconnected power system for a three-phase contingency at bus 9 without PSSs

Now considering the eigenvalues plot and analysis in Figure 7, Table 6 and Table 7, also considering the Figures 8, 9, 10 and 11, a suitable damping controller is required to mitigate the LFOs by increasing the system damping ratio of the EMs and thus enhanced the system stability status. The traditional practice by the utility is to install PSSs damping controllers on the system. However, the PSSs is a fixed parameter type under a specific operating condition and its parameters were obtained based on trial and error method. These have a considerable effect on its performance and may not effectively damp out the LFO in the system. For this study, an intelligent online PSSs parameter search based on the system condition is proposed using an FFA optimization algorithm and its performance is compared with other intelligent metaheuristics optimization methods for effectiveness comparison.

3.2.2 Parameter estimation via three-phase fault with FFA-PSS study

Now, the PSSs in the power system is equipped on the interconnected power system, and based on the proposed eigenvalue objective function and using the proposed FFA, the PSSs are designed for the interconnected power system based on the system operating conditions and compared with GA and PSO methods for robustness. A symmetrical three-phase fault is subjected to the system and with the proposed FFA based damping controller (PSSs) the LFOs were impressively mitigated and hence the system stability enhancement was achieved. Nonlinear time-domain simulation was performed and Figure 12 shows the stable generator relative power angles δ in radian for G_2 and G_3 relative to G_1 respectively for FFA-PSS while Figure 13 shows the stable generator field voltage E_{fd} in volts for G_1, G_2 and G_3 with FFA-PSS respectively. Similarly, Figure 14 shows stable the system active power response P_e in per unit for G_1, G_2 and G_3 respectively for the FFA based PSS while Figure 15 shows the stable system rotor speed response ω in radian per seconds for G_1, G_2 and G_3 respectively for the FFA-PSS.

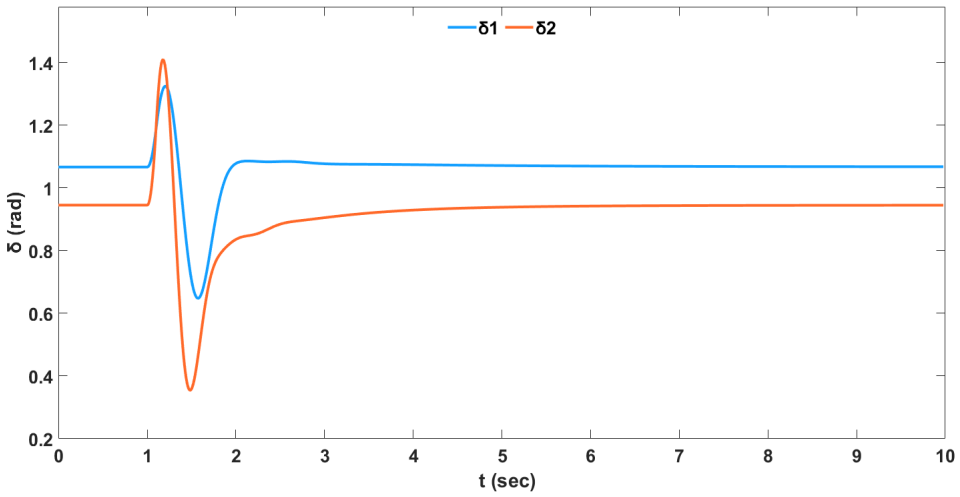

Figure 12. Stable relative power angle response w.r.t δ_1 of the interconnected power system for a three-phase fault at bus 9 with FFA-PSS

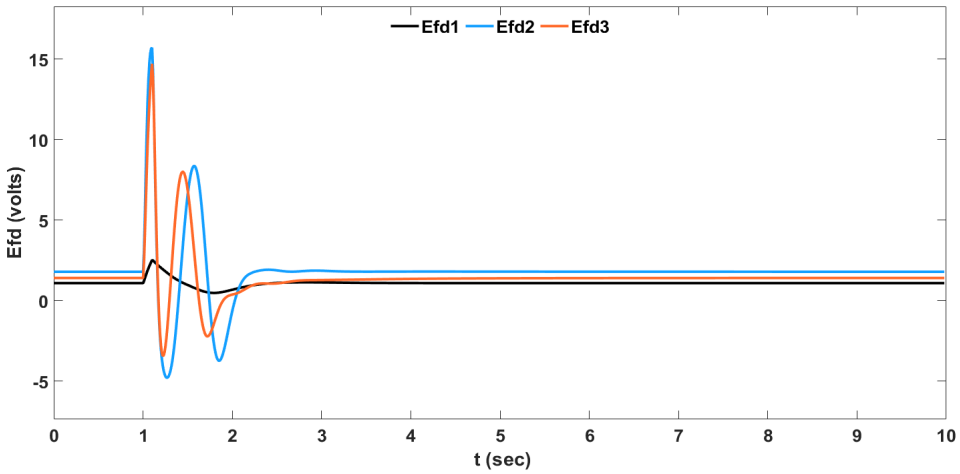

Figure 13. The stable field voltage response of the interconnected power system for a three-phase fault at bus 9 with FFA-PSS

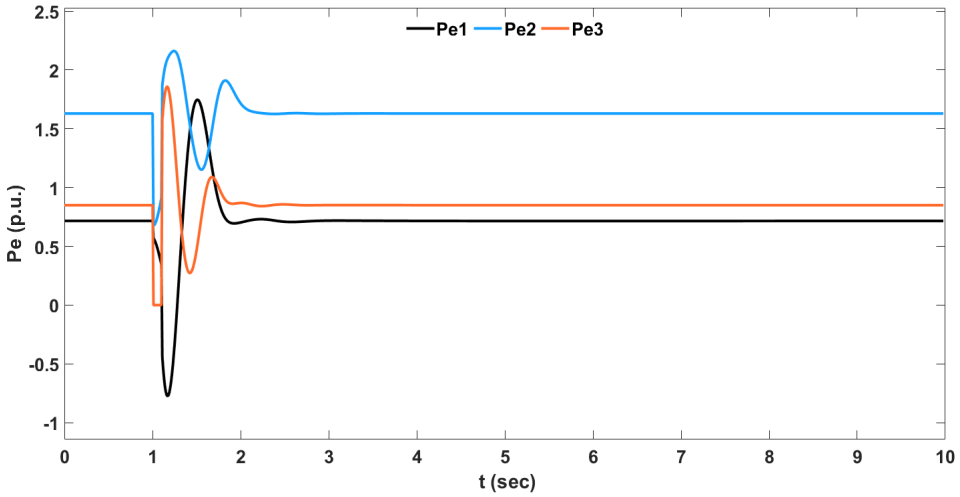

Figure 14. Stable active output power response of the interconnected power system for a three-phase fault at bus 9 with FFA-PSS

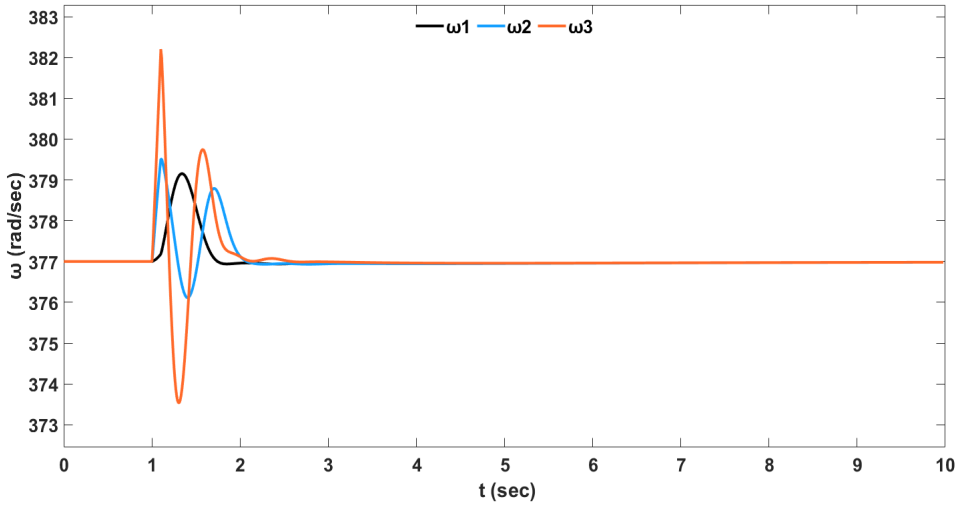

Figure 15. Stable rotor speed response of the interconnected power system for a three-phase fault at bus 9 with FFA-PSS

3.2.3 Proposed FFA based PSS design results comparison with GA-PSS and PSO-PSS

This section presents comparative simulation results for the PSS design between the GA-PSS, PSO-PSS, and the proposed FFA-PSS for LFOs robustness. Relative power angles δ in radian for G_2 $(\delta_2 - \delta_1)$ and G_3 $(\delta_3 - \delta_1)$ with respect to G_1 illustrates the system stability profile of the system using GA-PSS, PSO-PSS, and the proposed FFA-PSS design methods as shown in Figure 16 and Figure 17 respectively.

Similarly, Figure 18, Figure 19 and Figure 20 explains the active power output from G_1, G_2 and G_3 respectively using GA-PSS, PSO-PSS, and the proposed FFA-PSS design methods. The variation in the generator speeds for G_2 $(\omega_2 - \omega_1)$ and G_3 $(\omega_3 - \omega_1)$ relative to G_1 that corresponds to the system stability profile using GA-PSS, PSO-PSS and the proposed FFA-PSS design methods are shown in Figure 21 and Figure 22 respectively.

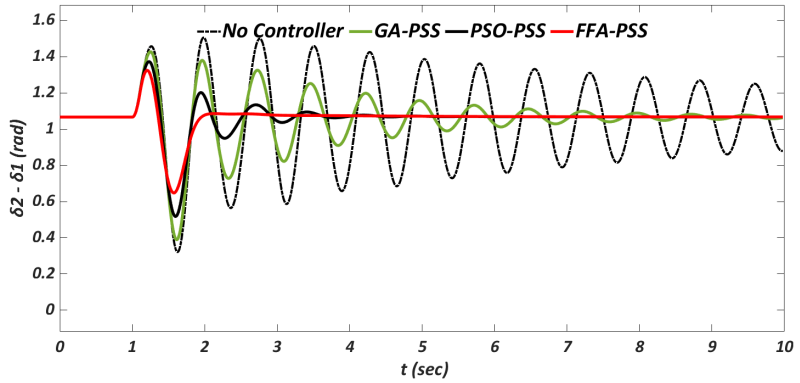

Figure 16. Relative power angle response of δ_2w.r.t to δ_1 for a contingency at bus 9 in the interconnected power system

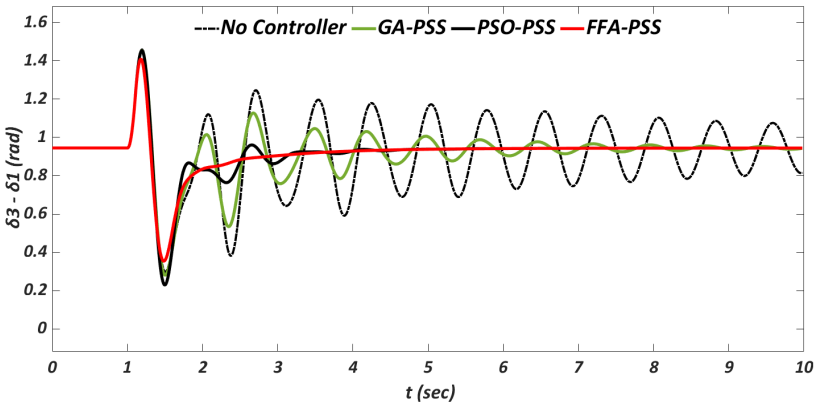

Figure 17. Relative power angle response of δ_3w.r.t to δ_1 for a contingency at bus 9 in the interconnected power system

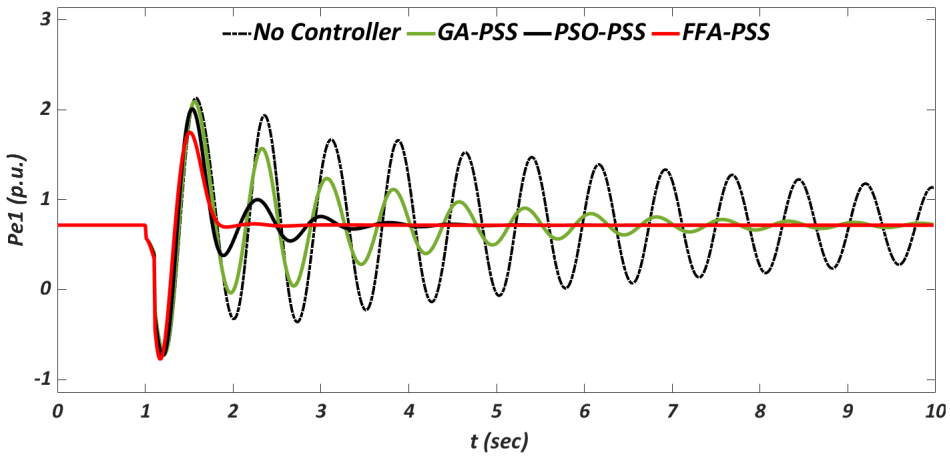

Figure 18. Active output power response of G1 for a contingency at bus 9 in the interconnected power system

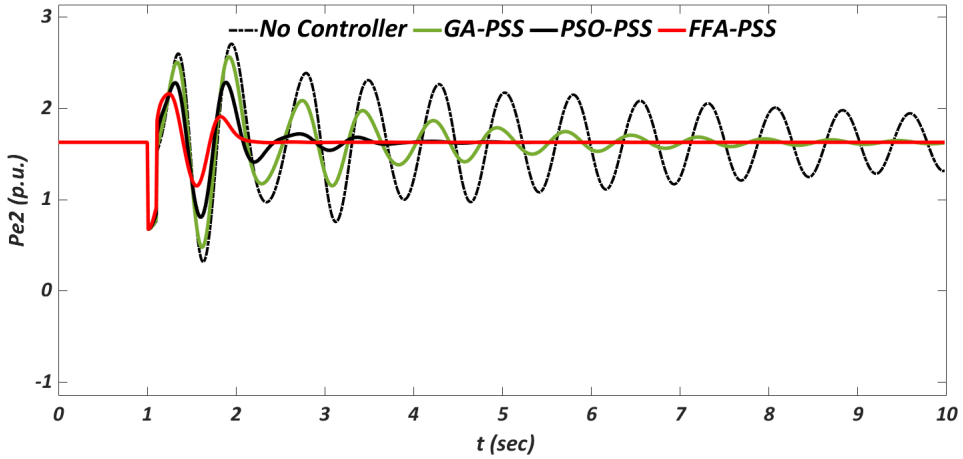

Figure 19. Active output power response of G2 for a contingency at bus 9 in the interconnected power system

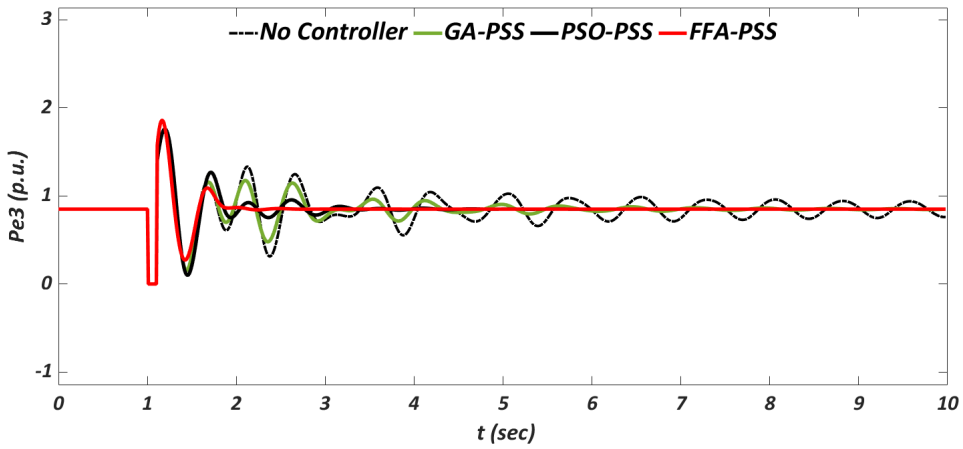

Figure 20. Active output power response of G3 for a contingency at bus 9 in the interconnected power system

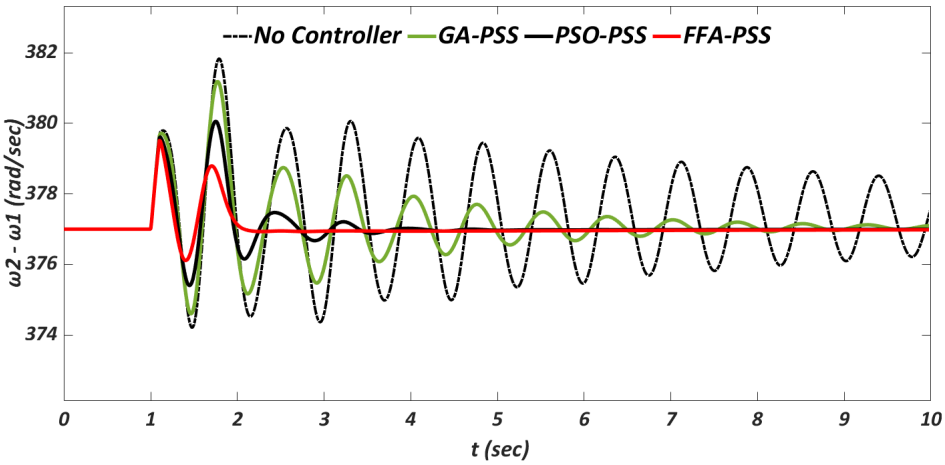

Figure 21. Rotor speed response of ω_2w.r.t to ω_1 for a contingency at bus 9 in the interconnected power system

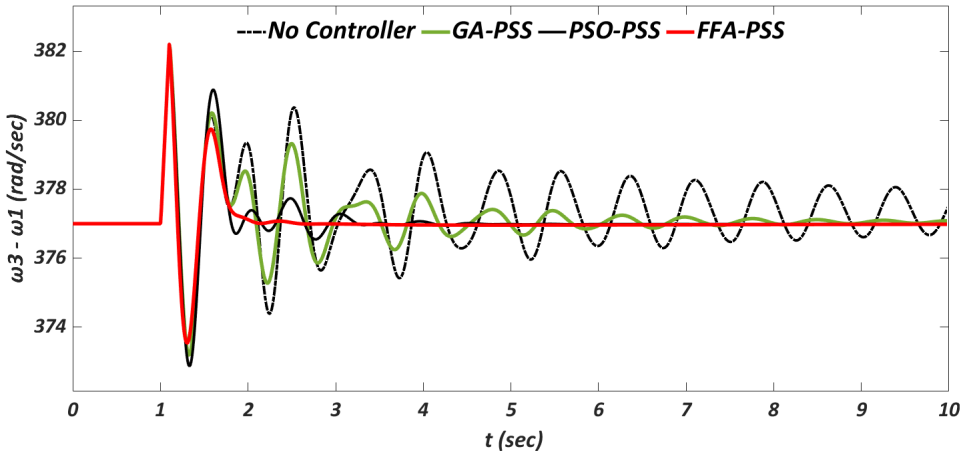

Figure 22. Rotor speed response of ω_3w.r.t to ω_1 for a contingency at bus 9 in the interconnected power system

From the time-domain simulation results, it was seen that the designed PSSs using the proposed FFA-PSS was effectively able to damp out the LFOs of the test system under a severe system disturbance. Thus, the FFA optimization algorithm can be applied as a general optimization method for the robust design of PSSs and other similar science and engineering optimization problems.

3.2.4 Transient Response Scenario for Controller Performance Analysis

This section explains the transient response simulation which describes the performance analysis of the interconnected power system when the system has no controller (NC), with GA-PSSs, PSO-PSSs, and the proposed FFA-PSSs for the 3 machines respectively. Table 8 considers how the Machine 1 plant responds to the transient situation with respect to settling time (ST), rise time (RT), peak time (PT), and peak magnitude (PM) for NC-PSSs, GA-PSS, PSO-PSS and FFA-PSS cases respectively. It is seen that, the ST response for ω_1 has remarkably improved by an amount of 82.68% for when the system has NC and with the proposed FFA-PSS controller respectively. Also, Table 9 shows for the Machine 2 system that, the ST response for ω_2 has remarkably improved by an amount of 79.48% for when the system has NC to with the proposed FFA-PSS controller respectively. Similarly, Table 10 explains for Machine 3 system how the ω_3 reacts ST for when the system has NC and when the FFA controller is used to design the PSS 3. The FFA controller was able to improve the system stability in terms of ST with an amount of 79.70% and thus damp out the LFOs under credible contingency.

The FFA controller in all the three machine transient simulation analyses was found able to improve the system stability in terms of ST, RT, PT, and PM with an acceptable amount compare with the other existing methods and thus damp out the LFOs under credible contingency. Nonetheless, the minimum control effort of the FFA-PSS controller exhibits its effectiveness to control LFOs and thereby enhancing the overall dynamic stability of the interconnected system as compared to the application of other non-intelligent and intelligent optimization techniques.

Table 8. Machine 1 transient performance

Cases	Machine 1															
	Settling Time (s)				Rise Time (s)				Peak Time (s)				|Peak Magnitude|			
	NC	GA	PSO	FFA	NC	GA $\times 10^{-4}$	PSO $\times 10^{-4}$	FFA $\times 10^{-4}$	NC	GA	PSO	FFA	NC	GA	PSO	FFA
ω_1	9.98	2.46	1.90	1.72	0.0857	74	69	108	1.39	1.34	1.34	1.34	379.5	379.1	379.1	379.1
δ_1	0	0	0	0	0	0	0	0	0	0	0	0	0.062	0.062	0.062	0.062
P_{e1}	9.89	2.023	2.287	1.818	0.025	0.24	0.23	0.24	1.58	1.51	1.52	1.51	2.12	1.73	1.74	1.74

Table 9. Machine 2 transient performance

Cases	Machine 2															
	Settling Time (s)				Rise Time (s)				Peak Time (s)				|Peak Magnitude|			
	NC	GA	PSO	FFA	NC	GA $\times 10^{-4}$	PSO $\times 10^{-4}$	FFA $\times 10^{-4}$	NC	GA	PSO	FFA	NC	GA	PSO	FFA
ω_2	9.99	2.32	2.29	2.04	0.0191	9.1	9.0	10	1.79	1.11	1.10	1.10	381.8	379.5	379.5	379.5
δ_2	9.91	3.05	3.03	3.14	0.029	69	70	80	1.98	1.21	1.21	1.21	1.505	1.331	1.331	1.324
P_{e2}	9.90	2.135	2.125	2.120	0.0025	0.0104	0.01	10	1.95	1.24	1.24	1.24	2.70	2.21	2.20	2.16

Table 10. Machine 3 transient performance

Cases	Machine 3															
	Settling Time (s)				Rise Time (s)				Peak Time (s)				|Peak Magnitude|			
	NC	GA	PSO	FFA	NC	GA $\times 10^{-4}$	PSO $\times 10^{-4}$	FFA $\times 10^{-4}$	NC	GA	PSO	FFA	NC	GA	PSO	FFA
ω_3	9.98	2.39	2.42	2.02	0.01	2.5	2.4	2.4	1.10	1.10	1.10	1.10	382.2	382.2	382.2	382.2
δ_3	9.89	4.30	4.31	4.30	0.016	0.15	0.45	0.5	1.19	1.18	1.18	1.18	1.459	1.399	1.402	1.409
P_{e3}	9.87	2.033	2.022	1.864	0.0007	0.0053	0.0050	0.0053	1.19	1.16	1.15	1.16	1.73	1.87	1.85	1.85

3.2.5 State of art the literature works comparison

State of the art literature works comparison is demonstrated in Table 11. The relative performance of accuracy for several PSSs tuning algorithms to obtain the optimal PSSs parameters for the three-phase disturbance in the system is made with all other current existing optimization approaches. The results in the list of references of Table 21 are fully comparable because the previous works compared here uses the same set of test case systems but only different PSS design methodology. Also, the results accuracy level was achieved on the same type of problem, fault subjected to the system and the same test systems but with different optimization methodology.

The result discloses that all the intelligent metaheuristic search algorithms were effective in designing the PSSs for SMIB and the interconnected multi-machine test power system. Among the various methods, the proposed FFA-PSS damping controller was found able to find the optimal PSSs parameters that can control the LFOs of the SMIB and multi-machine test system under a three-phase fault with an accuracy of 100%. Thus, the performance of proposed FFA over other techniques is promising in terms of convergence efficiency as compared to the state of the art literature work presented.

Table 11. Performance comparison with literature work

References	**PSS Tuning Method**	**Type of Fault considered**		
		LLLG	**FCT (s)**	**% Accuracy**
M. Singh et.al. [4]	Firefly Algorithm	✓	1.2	99.32
B. Hekimoğlu et.al.[5]	Grasshopper Optimization Algorithm	✓	1.2	100
E. L. Miotto et.al [9]	Novel Bat Algorithm	✓	1.2	99.36
B. Dasu et.al. [14]	Whale Optimization Algorithm	✓	1.2	99.678
S. Ekinci et.al. [15]	Salp Swarm Algorithm	✓	1.2	92.88
S. Ekinci et.al. [16]	Kidney-inspired Algorithm	✓	1.2	97.69
N. M. A. Ibrahim et.al. [17]	Bacterial Foraging Algorithm	✓	1.2	70
S. Ekinci et.al. [18]	Sine Cosine Algorithm	✓	1.2	98.06
D. Chitara et.al. [20]	Cuckoo Search Optimization Algorithm	✓	1.2	100
S. Ekinci et.al. [21]	Artificial Bee Colony Algorithm	✓	1.2	100
H. Beiranvand et.al [22]	General Relativity Search Algorithm	✓	1.2	100
Proposed Method	Farmland Fertility Algorithm	✓	1.2	100

* '✓' represents the occurrence of a fault

4. CONCLUSION

In this paper, a Power system stabilizer (PSS) is designed and applied for controlling Low-frequency oscillations (LFO) on WSCC 3-machine, 9-bus interconnected power system. The interconnected power system modeling for the small-signal and dynamic stability studies was conducted with and without PSSs on the system. By applying PSSs on the system, an intelligent metaheuristic based FFA optimization method was used to design the PSSs based on the system operating state. An eigenvalue based objective function was used in the optimization design problem which produced optimal PSSs parameters that forced the eigenvalues to drift to the left-hand side of the complex plane and thus stabilizing the system. The FFA method for PSSs design was compared with well-known GA and PSO existing intelligent metaheuristic optimization techniques for validation purposes. The eigenvalue analysis results show that the FFA based PSS provides improved damping ratio of the EMs and produces a solution with damping ratios greater than the GA-PSS and the PSO-PSS thus, impressively enhanced the system stability. Also, the phasor simulation results show that the transient responses of the system rise time, settling time, peak time and peak magnitude were all impressively improved by an acceptable amount for the interconnected system with the proposed FFA-PSS thus, was able to control the LFOs effectively and produces enhanced performance compared to the conventional GA and PSO based PSS. More so, the result validates the effectiveness of the proposed FFA tuned PSS for LFO control which demonstrates robustness, efficiency, and convergence speed ability than the classical GA and PSO tuning methods.

ACKNOWLEDGMENT

This research was supported by GPB-UPM under Grant No. 9630000, University Putra Malaysia (UPM) through Advanced Lightning, Power, and Energy Research (ALPER).

REFERENCES

[1] V. Veerasamy *et al.*, A novel discrete wavelet transform-based graphical language classifier for identification of high-impedance fault in distribution power system, *International Transactions on Electrical Energy Systems,* February, 2020, 1–24.

[2] M. Saadatmand, B. Mozafari, G. B. Gharehpetian and S. Soleymani, Optimal PID controller of large-scale PV farms for power systems LFO damping, *International Transactions on Electrical Energy Systems*, February, 2020, 1–14.

[3] G. Tu, Y. Li, J. Xiang and J. Ma, Distributed power system stabiliser for multimachine power systems, *IET Generation, Transmission & Distribution,* 13(5), 2019, 603–612.

[4] M. Singh, R. N. Patel and D. D. Neema, Robust tuning of excitation controller for stability enhancement using multi-objective metaheuristic firefly algorithm, *Swarm and Evolutionary Computation*, 44, 2019, 136–147.

[5] B. Hekimoğlu, Robust fractional order PID stabilizer design for multi-machine power system using grasshopper optimization algorithm, *Journal of the Faculty of Engineering and Architecture of Gazi University*, 35(1), 2020, 165–180.

[6] A. Faraji and A. Hesami Naghshbandy, A combined approach for power system stabilizer design using continuous wavelet transform and SQP algorithm, *International Transactions on Electrical Energy Systems*, 29(3), 2019, 1–18.

[7] A. K. Gupta, K. Verma and K. R. Niazi, Robust coordinated control for damping low frequency oscillations in high wind penetration power system, *International Transactions on Electrical Energy Systems*, 29(5), 2019, 1–17.

[8] A. Sabo, N. Izzri and A. Wahab, Rotor angle transient stability methodologies of power systems: A comparison, *IEEE Student Conference on Research and Development (SCOReD)*, Malaysia, 2019, 1–6.

[9] E. L. Miotto, P. B. De Araujo, E. D. V. Fortes, B. R. Gamino, L. Fabiano and B. Martins, Coordinated tuning of the parameters of pss and pod controllers using bioinspired algorithms, *IEEE Transactions on Industry Applications*, 54(4), 2018, 3845–3857.

[10] H. Verdejo, R. Torres, V. Pino, W. Kliemann, C. Becker and J. Delpiano, Tuning of controllers in power systems using a heuristic-stochastic approach," *Energies*, 12(12) 2325, 2019, 1–25.

[11] M. Jokarzadeh, M. Abedini, and A. Seifi, Improving power system damping using a combination of optimal control theory and differential evolution algorithm, *ISA Transactions*, 90, 2019, 169–177.

[12] T. Guesmi, A. Farah, H. H. Abdallah and A. Ouali, Robust design of multimachine power system stabilizers based on improved non-dominated sorting genetic algorithms," *Electrical Engineering*, 100(3), 2018, 1351–1363.

[13] D. Wang, N. Ma, M. Wei and Y. Liu, Parameters tuning of power system stabilizer PSS4B using hybrid particle swarm optimization algorithm, *International Transactions on Electrical Energy Systems*, 28(9), 2018, 1–17.

[14] B. Dasu, M. Sivakumar and R. Srinivasarao, Interconnected multi-machine power system stabilizer design using whale optimization algorithm, *Protection and Control of Modern Power Systems*, 4(2), 2019, 1–11.

[15] S. Ekinci and B. Hekimoğlu, Parameter optimization of power system stabilizer via salp swarm algorithm, *5th International Conference on Electrical and Electronic Engineering (ICEEE 2018)*, Istanbul, Turkey, 2018, 143–147.

[16] S. Ekinci, A. Demiroren, and B. Hekimoglu, Parameter optimization of power system stabilizers via kidney-inspired algorithm, *Transactions of the Institute of Measurement and Control*, 41(5), 2019, 1405–1417.

[17] N. M. A. Ibrahim, B. E. Elnaghi, H. A. Ibrahim and H. E. A. Talaat, Performance assessment of bacterial foraging based power system stabilizer in multi-machine power system, *International Journal of Intelligent Systems and Applications*, 11(7), 2019, 43–53.

[18] S. Ekinci, "Optimal design of power system stabilizer using sine cosine algorithm, *Journal of the Faculty of Engineering and Architecture of Gazi University*, 34(3), 2019, 1329–1350.

[19] L. Chaib, A. Choucha and S. Arif, Optimal design and tuning of novel fractional order PID power system stabilizer using a new metaheuristic bat algorithm, *Ain Shams Engineering Journal*, 8, 2017, 113–125.

[20] D. Chitara, K. R. Niazi, A. Swarnkar and N. Gupta, Cuckoo search optimization algorithm for designing of a multimachine power system stabilizer, *IEEE Transactions on Industry Applications*, 54(4), 2018, 3056–3065.
[21] S. Ekinci and A. Demiroren, Modeling, simulation, and optimal design of power system stabilizers using ABC algorithm, *Turkish Journal of Electrical Engineering & Compututer Sciences*, 24, 2016, 1532–1546.
[22] H. Beiranvand and E. Rokrok, General relativity search algorithm: A global optimization approach, *International Journal of Computational Intelligence and Applications*, 14(3), 2015, 1550017 (29 pages).
[23] H. Shayanfar and F. S. Gharehchopogh, Farmland fertility: A new metaheuristic algorithm for solving continuous optimization problems, *Applied Soft Computing*, 71, 2018, 728–746.
[24] A. A. Z. Diab, S. I. El-ajmi, H. M. Sultan and Y. B. Hassan, Modified farmland fertility optimization algorithm for optimal design of a grid-connected hybrid renewable energy system with fuel cell storage: case study of Ataka, Egypt, *International Journal of Advanced Computer Science and Applications*, 10(8), 2019, 119–132.
[25] D. Mondal, A. Chakrabarti and A. Sengupta, *Power System Small Signal Stability Analysis and Control*. New York, USA: Academic Press, 2014.
[26] H. Beiranvand and E. Rokrok, MatSim: A Matpower and simulink based tool for power system dynamics course education, *31th Power System Conference,* Tehran, Iran, 2016, 1–6.
[27] P. W. Sauer, M. A. Pai and J. H. Chow, *Power System Dynamics and Stability With Synchrophasor Measurement and Power System Toolbox*, USA: Wiley-IEEE Press*,* 2018.